

Crystal Structure of Stoichiometric $\text{YBa}_2\text{Fe}_3\text{O}_8$ Pavel Karen,^{*,†} Emmanuelle Suard,[‡] and François Fauth[§]

University of Oslo, P.O. Box 1033 Blindern, N-0315 Oslo, Norway, Institute Max von Laue and Paul Langevin, BP 156, 38042 Grenoble, France, and European Synchrotron Radiation Facility, BP 220, 38043 Grenoble, France

Received September 7, 2004

The oxygen-nonstoichiometry locus in $\text{YBa}_2\text{Fe}_3\text{O}_{8+w}$ changes with the sign of w . The singularity at $w = 0$ is studied by Rietveld refinement of combined high-resolution, high-intensity neutron and synchrotron X-ray diffraction data collected at room temperature on red-colored stoichiometric $\text{YBa}_2\text{Fe}_3\text{O}_8$. A residual disorder of oxygen atoms is identified in a concentration of 0.03 vacancy/interstitials per formula, with corresponding anisotropy in thermal displacements of oxygen neighbors. The disorder improves accommodation of trivalent iron over the two unequal coordination polyhedra and is not identical with the charged Frenkel disorder induced thermally. The symmetry of the cooperative magnetic order is $Ib'am$, with opposite moments of equal magnitude ($4.07 \mu_B$ at 295 K) at the two iron sites.

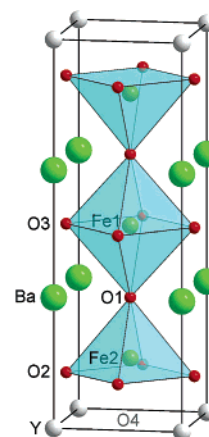


Figure 1. Unit cell of $\text{YBa}_2\text{Fe}_3\text{O}_8$, space group $P4/mmm$.

$\text{YBa}_2\text{Fe}_3\text{O}_8$ is the hitherto only triple-perovskite analogue of $\text{YBa}_2\text{Cu}_3\text{O}_7$ where copper is fully replaced by another transition metal. These two phases actually have a wide miscibility gap,¹ owing to the inability of iron to adopt square-planar coordinations in oxides. Consequently, Fe^{III} is stabilized in one octahedral and two square-pyramidal environments per unit cell, leading to the $\text{YBa}_2\text{Fe}_3\text{O}_8$ composition (Figure 1).²

Accordingly, the redox-driven oxygen-nonstoichiometry range is centered on trivalent iron, instead of extending between integer valences of the two sites as in the cuprate. The $\text{YBa}_2\text{Fe}_3\text{O}_{8+w}$ homogeneity range is narrower but still considerable. At 900 °C, it spans from the lower stability limit of $w \approx -0.25$ to at least $w = +0.08$, which is achieved by oxygen saturation at 1 bar without the actual upper stability limit being crossed.³ The oxidized $\text{YBa}_2\text{Fe}_3\text{O}_{8+w}$ ($w > 0$) of a very dark brown/violet color is formed in diluted oxygen atmospheres. With reductions below $w = 0$ generally requiring diluted hydrogen and CO/CO_2 mixtures being out

of the question for a Ba-containing oxide, stoichiometric $\text{YBa}_2\text{Fe}_3\text{O}_8$ belongs to the gray zone between diluted oxygen and hydrogen. Neutron powder diffraction (NPD) of the readily obtainable oxidized and reduced phases revealed that the structural locus for the oxygen nonstoichiometry depends on the sign of w . Whereas oxygen vacancies ($w < 0$) are formed in the O3 sites of the Fe1 coordination octahedron, the added oxygen ($w > 0$) is accommodated as O4 in the Fe2 coordination sphere. Extrapolation of this result to the stoichiometric phase would represent a special Frenkel-defect situation, in which the vacancies and interstitials that are simultaneously present when $w = 0$ would not be accommodated randomly but have their respective preferences for the Fe1 and Fe2 coordinations.

In an attempt to assess this possibility, stoichiometric $\text{YBa}_2\text{Fe}_3\text{O}_8$ was synthesized by controlled deoxidation of the oxygen-saturated phase ($w = 0.08$) with a precise amount of metallic Ce as a getter in a sealed evacuated (100 Pa) silica ampule. The ampule of ~ 10 mL volume was held at 550 °C over a period of 2 weeks. The method yielded approximately 1.5 g of a sample with impeccable homogeneity across the bulk, judged by its bright red/brown color, sharp symmetrical Bragg reflections, and no deviations from iron trivalence detected beyond the typical standard error of $\Delta w = \pm 0.003$ by both direct and inverse titration with Ce^{IV} . The strategy for the occupancy assessment was to make a combined Rietveld refinement of high-flux NPD data, collected at the recently upgraded “super”-high-resolution

* To whom correspondence should be addressed. E-mail: pavel.karen@kjemi.uio.no. Phone: +47 228 555 90.

[†] University of Oslo.

[‡] Institute Max von Laue and Paul Langevin.

[§] European Synchrotron Radiation Facility.

(1) Karen, P.; Andresen, P. H.; Kjekshus, A. *J. Solid State Chem.* **1992**, *101*, 48.

(2) Huang, Q.; Karen, P.; Karen, V. L.; Kjekshus, A.; Lynn, J. W.; Mighell, A. D.; Rosov, N.; Santoro, A. *Phys. Rev. B* **1992**, *45*, 9611.

(3) Linden, J.; Kjekshus, A.; Karen, P.; Miettinen, J.; Karppinen, M. *J. Solid State Chem.* **1998**, *139*, 168.

two-axis D2B diffractometer (128 position-sensitive ^3He counters) at the ILL Grenoble, with synchrotron X-ray powder diffraction (SXPd) data of high resolution, collected at the high-flux beamline ID31 (nine parallel Si analyzer/scintillation-counter detector units) of the ESRF Grenoble. The NPD sample of ~ 0.5 g was enclosed in a vanadium container, the SXPd sample (0.005 g) was sealed in a 0.375-mm-diameter glass capillary. Data acquisitions at 295–297 K were performed over redundant angular ranges 2θ so that the counting statistic was constant along the actually used intervals (NPD, 150° wide, in steps of 0.05° ; SXPd, 2 – 50° wide, in steps of 0.002°). Two sets of NPD data were collected on two occasions, for 6 h each, with wavelength $\lambda_{\text{neutron}} \approx 1.59$ Å. The SXPd data were collected with $\lambda_{\text{X-ray}} = 0.499\,797(5)$ Å for 3 h under progressive scaling of the counting time toward higher angles.

Because $\text{YBa}_2\text{Fe}_3\text{O}_8$ is an antiferromagnet with a Néel temperature of ~ 660 K,^{4,5} neutron scattering from ordered magnetic moments was present in the NPD data. As established in ref 2, the magnetic cooperative order is of the Wollan–Koehler⁶ G-type, characterized by alternating polarity of the moments in all three directions. Such an arrangement, built on the nuclear cell of the $P4/mmm$ space group (Figure 1), suggests doubling of the unit-cell vectors upon an $F4/mmc$ symmetry, the true Bravais lattice of which dictates $I4/mcm$. Because the ordered spins are confined in the a/b plane, the 4-fold axis is removed and the symmetry of the nuclear arrangement in the magnetic cell becomes $Ibam$. The anti-operations of symmetry that reflect correctly the orientations of the magnetic moments are then represented by the magnetic group $Ib'am$, listed as no. 541 in the Shubnikov-group tables⁷ and having the same symbol in the Opechowski–Guccione notation⁸ listed⁹ as no. 632 by Litvin. This symmetry group respects the fact that no nuclear sites are split by the magnetic order. In cases when refinements of magnetic and nuclear structures are performed on two different cells, this may be per convenience violated, and the present symmetry analysis sets straight such a simplified approach used previously for $\text{YBa}_2\text{Fe}_3\text{O}_8$.^{2,5} The magnetic unit cell of the ideally stoichiometric $\text{YBa}_2\text{Fe}_3\text{O}_8$ phase is drawn in Figure 2, with lattice vectors related to those of the nuclear cell by the transformation matrix $(1\bar{1}0/110/002)$.

Rietveld refinements of the combined NPD and SXPd patterns were performed in the GSAS software suite.¹⁰ Bragg reflections from vanadium of the sample container have been included in the NPD pattern fit. Two phase impurities were identified in the SXPd pattern: a cubic perovskite ($a = 4.1630$ Å) with a refined mass fraction of 0.023(1) and the orthorhombic BaFe_2O_4 with a mass fraction of 0.0071(3).

- (4) Karen, P.; Kjekshus, A. J. *Solid State Chem.* **1994**, *112*, 73.
 (5) Karen, P.; Kjekshus, A.; Huang, Q.; Karen, V. L.; Lynn, J. W.; Rosov, N.; Sora, I. N.; Santoro, A. J. *Solid State Chem.* **2003**, *174*, 87.
 (6) Wollan, E. O.; Koehler, W. C. *Phys. Rev.* **1955**, *100*, 545.
 (7) Koptsiik, V. A. *Shubnikovskie gruppy*; Izdatelstvo Moskovskogo Universiteta: Moscow, 1966; p 329.
 (8) Opechowski, W.; Guccione, R. In *Magnetism*; Rado, G. T., Suhl, H., Eds.; Academic Press: New York, 1965; Vol. 2A, pp 105–165.
 (9) Litvin, D. B. *Acta Crystallogr., Ser. A* **2001**, *57*, 729.
 (10) Larson, A. C.; Von Dreele, R. B. *General Structure Analysis System (GSAS)*; Los Alamos National Laboratory Report LAUR 86-748 (version 2004 used); Los Alamos National Laboratory: Los Alamos, NM, 2004.

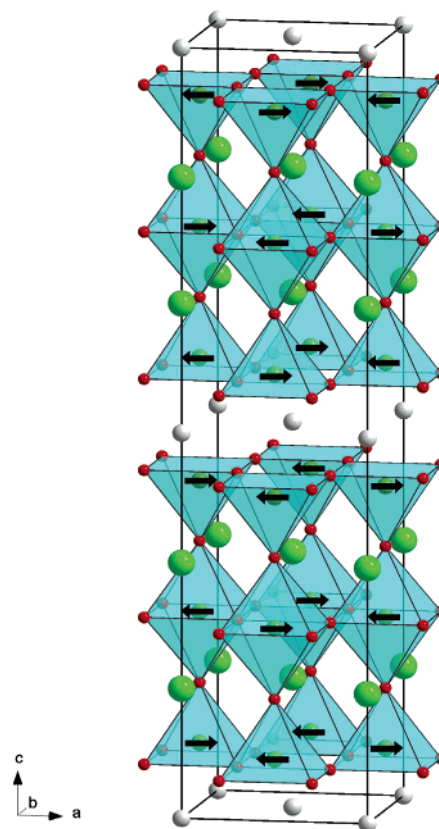


Figure 2. Magnetic unit cell of $\text{YBa}_2\text{Fe}_3\text{O}_8$, magnetic group $Ib'am$.

Considering the relatively large unit-cell parameter of the former phase, its identity was assumed (for the purpose of the Rietveld refinement) to be of a disordered cubic oxide–carbonate related to the triple perovskite $\text{Ba}_3\text{Y}_2(\text{CO}_3)\text{O}_5$ ^{11,12} rather than a BaFeO_3 -based solid solution.¹ Such an oxide–carbonate is likely to have been formed during the oxygen–content control in the closed system. Formation of the impurity phases may correspond to a small excess of Ba in the starting mixture. Occupancy refinements of the metal sites suggest that $\text{YBa}_2\text{Fe}_3\text{O}_8$ is a point compound with respect to the metal atoms.

An overall release of site occupancies, together with isotropic thermal displacements, provided the following values: 1.014 Y, 1 Ba (fixed), 0.988 Fe1, 0.994 Fe2, 1.004 O1, 1.043 O2, 1.053 O3, and 0.033 O4. When metal occupancies were fixed to unity, oxygen occupancies did not change significantly, viz., remained larger than 1.000 for O2 and O3. A trial occupancy refinement of O4 alone yielded 0.062(5) with a clear detriment to $R(F^2)$ in all three patterns, suggesting that fixing the occupancies to 1 is incorrect for O2 and O3. A stoichiometry constraint was therefore adopted that relates the O4 occupancy to a compensating vacancy content at the O2 and O3 sites, yielding 0.028(5) for O4 versus 1.002(2) and 0.982(3) for O2 and O3, respectively. The O2 occupancy was fixed to unity with no detriment in figures of merit, and the subsequent refinement of the O4 and O3 occupancies, thus constrained in a Frenkel-type anti-

- (11) Karen, P.; Braaten, O.; Fjellvåg, H.; Kjekshus, A. In *AMSAHTS '90*, NASA Conference Publication 3100; NASA: Hammon, MD, 1991; p 117.
 (12) Zhang, W.; Osamura, K. *Mater. Trans., JIM* **1991**, *32*, 1048.

Table 1. Refined Atomic Parameters of Nuclear [$a = 3.91792(0)$ Å, $c = 11.82444(2)$ Å, $P4/mmm$] and Magnetic [$a = b = 5.54078(1)$ Å, $c = 23.64888(3)$ Å, $Ib'am$] Cells

	Y	Ba	Fe1	Fe2	O1	O2	O3	O4
<i>P4/mmm</i> Wyckoff site	1a	2g	1d	2h	2h	4i	2e	1c
<i>x</i>	0	0	1/2	1/2	1/2	0	0	1/2
<i>y</i>	0	0	1/2	1/2	1/2	1/2	1/2	1/2
<i>z</i>	0	0.33644(4)	1/2	0.15992(7)	0.31558(14)	0.11832(8)	1/2	0
occupancy	1	1	1	1	1	1	0.985(2)	0.030(4)
<i>Ib'am</i> Wyckoff site	4c	8h	4b	8i	8i	16k	8e	4d
<i>x</i>	0	0	1/2	1/2	1/2	1/4	1/4	1/2
<i>y</i>	0	0	0	0	0	1/4	1/4	0
<i>z</i>	0	0.16822(2)	1/4	0.07996(3)	0.15779(7)	0.05916(4)	1/4	0
$100U_{\text{iso}}$ (Å ²)	0.23(2)	0.38(1)	0.36(2)	0.23(1)	0.69(3)	0.66(2)	0.12(3) ^a	0.12(3) ^a
M_x (μ _B)			−4.07(3) ^b	4.07(3) ^b				

^a Constrained equal. ^b Constrained equal; when free, the (large) standard deviations overlap.

site disorder, gave the best $R(F^2)$ of all occupancy models. Trials with Y/Ba or Y/Fe anti-site defects did not improve the overall $R(F^2)$ in the combined refinement. Testing SXPd data alone in this matter was inconclusive owing to correlations with oxygen occupancies. A standalone NPD refinement yielded occupancy $-0.003(12)$ for Y at the Ba site and $-0.006(25)$ for Ba at the Y site (together with about 0.060 O4 interstitials and 0.030 O3 vacancies). The practical absence of anti-site mixing is also expected from the large difference in ionic sizes and is in accordance with experimental data on other iron oxides.¹³

The combined refinement, with the Frenkel-type anti-site disorder of oxygen implemented, suggests 0.030(4) for the content of the “interstitial” oxygen O4, compensated for by the same amount of O3 vacancies per the $\text{YBa}_2\text{Fe}_3\text{O}_8$ formula. The figures of merit for the SXPd, NPD1, and NPD2 patterns in the combined refinement were as follows: $R_p = 0.0540, 0.139,$ and 0.0179 and $R(F^2) = 0.0408, 0.0260,$ and 0.0393 for 1784, 1037, and 1003 reflections, respectively. The overall χ^2 was 3.689 for 152 variables. The refined atomic parameters for both the nuclear and magnetic structures of $\text{YBa}_2\text{Fe}_3\text{O}_8$ are listed in Table 1.

Trial releases of anisotropic thermal displacements show no correlations of these with other refined variables but also no improvement in $R(F^2)$. With the possible exception of O1 and O2, all atoms vibrate rather isotropically. Anisotropic displacements were accordingly not released for the final refinement listed in Table 1. Of the two exceptions, O2 appears to have a large amplitude along c ($U_{33} = 0.0085$ Å², whereas $U_{11} = 0.0044$ Å² and $U_{22} = 0.0057$ Å²) and O1 a large amplitude within the a/b plane ($U_{11} = U_{22} = 0.0088$ Å², whereas $U_{33} = 0.0035$ Å²). These displacements would be consistent with the presence of the added “interstitial” O4 atoms pushing O2 along c and with the presence of O3 vacancies changing the Fe1 octahedra into deformed square pyramids.

Although such local shifts cannot be implemented in bond-valence calculations, the latter still provide important clues about the structure. As can be seen from Table 2, the iron–oxygen bond distances are stretched to their limits in both extremes to ensure that the unequal polyhedra host iron atoms with valences as equal as possible. The same task is being

Table 2. Calculated Interatomic Distances (in Å) and Bond-Valence Sums (BVS; Parameters from Reference 18) in $\text{YBa}_2\text{Fe}_3\text{O}_8$ Coordination Polyhedra

atom	Y	Ba	Fe1	Fe2	BVS
O1		2.7813(2)	2.1807(17)	1.8405(24)	2.168(7)
O2	2.4073(6)	3.287(12)		2.0198(4)	1.841(3)
O3		2.7528(4)	1.9590(0)		2.260(4)
O4	2.7704(0)			1.8910(8)	0.058(8)
BVS	2.817(6)	2.462(3)	2.935(8)	2.800(10)	

fulfilled by the oxygen vacancy and interstitial formation in the coordination spheres of Fe1 and Fe2, respectively, in a demonstration of Pauling’s parsimony rule.¹⁴ In addition, the vacancy/interstitial disorder relieves the strong overbonding of the Ba atom.

True intrinsic Frenkel defects¹⁵ as pairs of charged interstitials and vacancies are rarely if ever detected by diffraction methods because their concentrations are low and their distribution random. According to point-defect modeling of the oxygen-exchange equilibria between $\text{YBa}_2\text{Fe}_3\text{O}_8$ and O_2 ,¹⁶ temperatures in excess of 1000 K are needed for concentrations of the intrinsic defects of the O_i'' and V_O'' type (in Kröger–Vink notation¹⁷) to exceed values obtained from the present Rietveld refinements of the room-temperature diffraction data.

The explanation of this disagreement relates the refined concentrations to a ground-state content of noncharged structural defects at their two separate loci, in principle an intersite disorder of oxygen atoms, in which the trivalence of iron is maintained by structural distortions. Charged defects, in contrast, are formed by thermal excitations on top of such structural defects and would be coupled to the formation of redox species of iron (often referred to as holes and electrons). Because Frenkel refers to charged “dissociated” defects in his paper¹⁵ about thermally activated transport, the term Frenkel defect for the noncharged defect situation in $\text{YBa}_2\text{Fe}_3\text{O}_8$ is appropriate only as a parable.

Supporting Information Available: GSAS-generated CIF file of the refined powder diffraction data. This material is available free of charge via the Internet at <http://pubs.acs.org>.

IC048746B

(13) Chlan, V.; Štěpánková, H.; Procházka, V.; Englich, J.; Kohout, J.; Nižňanský, D.; Buršík, J. *J. Magn. Magn. Matter.* **2005**, *290–291*, 993.

(14) Pauling, L. *J. Am. Chem. Soc.* **1929**, *51*, 1010.

(15) Frenkel, J. *Z. Phys.* **1926**, *35*, 652.

(16) Karen, P. Unpublished.

(17) Kröger, F. A.; Vink, H. *J. Solid State Phys.* **1956**, *3*, 307.

(18) Brown, I. D. *The Chemical Bond in Inorganic Chemistry, The Bond Valence Model*; Oxford University Press: Oxford, U.K., 2002; pp 225–226.